Emission Spectroscopy on Pyrotechnic Mixtures

Sebastian Knapp*, Christian Günthner, Stefan Kelzenberg, Evelin Roth, Angelika Raab, Volker Weiser

Fraunhofer-Institut für Chemische Technologie ICT, 76327 Pfinztal, Germany

sebastian.knapp@ict.fraunhofer.de

Keywords: Pyrotechnic Mixture, Emission Spectroscopy, Modeling

ABSTRACT

Pyrotechnic mixtures mostly consist of systems of fuel and oxidizer particles with defined mixture ratios and particle sizes. After ignition by a defined energy input, they react highly exothermic with a high energy release in a combustion process and produce a bright shining reaction zone with light emission from UV till the far MIR. Especially for colorful emission and high temperatures, metals or metal compounds are used. Emission spectroscopy is a well-known experimental measurement technique to examine the reaction zone and burning behavior of such mixtures. By analyzing the resulting emission spectra, valuable information can be obtained: the intermediate and end product occurrence, the particles' surface and gas phase temperature, the emissivity, the radiation of energy, the CIE-color, and the reaction mechanism. In the case of pyrotechnic mixtures, most of this information can be received from the emitted light in the UV/VIS wavelength range. In the gas phase of the reaction, the intermediate products, e.g. atoms and diatomic molecules, emit because of a stimulated electronic transition. In the UV/VIS wavelength range, they show atomic lines and diatomic molecule band systems. The background emission is usually gray body radiation of the solid particles. Because of the high temperature, the maximum of the gray body function is in the near-infrared wavelength range and therefore, it is still visible in the UV/VIS range.

A valuable experimental device to investigate pyrotechnic mixtures is a window bomb. At ICT, a color high-speed camera and a fast grating UV/VIS spectrometer are used to monitor the reaction process. The window bomb is a chimney type high pressure autoclave, which can be operated with different gases and pressured up to 15 MPa. For the correction of the intensity ratios of atomic lines and diatomic molecule band systems and to obtain information about the radiated energy, an intensity calibration is necessary. It corrects for different sensitivities of the detector and correlates the measured intensities with the radiance. The calibration was realized using a calibrated light source with known radiation, in our case a Tungsten strip lamp. In addition, the optical setup was adapted to limit the view angle.

By analyzing the received UV/VIS spectra of the experiments, the chronological occurrence of different species can be reconstructed. The gas phase temperature and the molecules emissivity can be obtained by modeling the spectrum from the atomic lines and the diatomic molecule band systems.

In this work, we present how emission spectra are obtained in the UV/VIS range, as well as how the spectra are analyzed. We demonstrate the technique in various examples.

Introduction

Pyrotechnic mixtures mostly consist of systems of fuel and oxidizer particles with defined mixture ratios and particle sizes. After ignition by a defined energy input, they react highly exothermic with a high energy release in a combustion process and produce a bright shining reaction. Actually, this type of reaction is of widespread interest to rapidly produce large amounts of heat at high temperature levels and has found many applications [1][2]. Pyrotechnic mixtures are used for welding process which is still the most frequently used method for welding of railroad tracks [3]. They are also used to purify ores of some metals (e.g. uranium). Recently the preparation of ceramics becomes more important [4]. Due to the large heat release and its self-sustaining nature, pyrotechnic mixtures have been used in warheads as incendiary devices [5]. As a big advantage most mixtures are very insensitive concerning shock and friction.

Currently, numerous investigations on pyrotechnic reactions are done using different metals and oxidizers [6] studying burning rates [7], influence of particle size [8] and pressure [9][10]. However, the physico-chemical mechanisms of pyrotechnic reactions are still far from being completely understood. Therefore, the modeling is also of particular interest [11] and there are some preliminary approaches for it [12], which describe particle ignition and propagation of reaction fronts in porous energetic materials [13]-[17]. Experimentally, different measurement methods are used for analyzing pyrotechnic mixture combustion. Here, the emission spectroscopy in the UV/VIS range will be discussed. In the visible (VIS) till infrared (IR) range a continuum can occur, emitted by hot particles or a hot surface of a condensed phase material. It can be assumed to emit gray body radiation where the function of a gray body can be fitted to the experimental spectrum to get the continuum temperature. By two photodiodes with different sensitivity ranges a very simple setup for continuum temperature can be built up, the 2-color pyrometer. Gray body temperature can be also measured in the near-infrared wavelength range (NIR). In the VIS range, discrete lines and band spectra are often emitted by electronically excited atoms and diatomic molecules in the vapor phase. They are formed in the reaction zone and allow a temperature determination of this zone. Comparison of the diatomic spectra with calculated ones gives the possibility to determine the temperature of the reaction zone without limitations. Calculation of intensity distribution of molecule bands is possible under the assumption that the atoms and molecules were in thermal equilibrium so that the energy levels were populated according to the Boltzmann statistic. The necessary transition probabilities for the occupied vibrational states can be found in literature or calculated from the diatomic constants also available in literature [18]. Previous work has shown that in many cases a good agreement between calculated and experimental spectra can be achieved [19]-[22]. The spectroscopic methods base on the modelling of these spectra and on the comparison of measured intensity distribution with calculated one.

In this work the arising intermediate diatomic species, particle and reaction zone temperature of the Al/CuO thermite reaction was investigated in different experiments to get indications of the reaction mechanism. From the determined grey body temperature, which is the particle surface temperature, absolute intensities can be derived to obtain information about radiated energy and the emissivity. In the UV/VIS range the upcoming diatomic molecules were identified and their occurrence was analyzed. On the basis of modelling the diatomic molecule band systems, the gas phase temperature of the reaction was determined.

Modelling

GREY BODY RADIATION

For temperature measurement with 2-color-pyrometry and NIR-spectrometer, the emission of solid surfaces or particles, the grey body radiation, is used. The grey body describes the continuous emission or absorption from solid surfaces which is based on the radiance L describing black body radiation:

$$L_{\lambda B}(\lambda,T)=\frac{c_1}{\lambda^5\left(\exp\left(\frac{c_2}{\lambda T}\right)-1\right)}$$

With $c_1 = 2\pi hc^2 = 3.7415\cdot 10^{-12}\,\mathrm{W\,cm^2}$ and $c_2 = hc/k_B = 1.43879\,\mathrm{cm\,K}$. λ is the wavelength and T the temperature. A black body is an idealized physical body that absorbs all incident electromagnetic radiation, regardless of frequency or angle of incidence [23]. For real samples the law has to be modified by an emissivity ε depending on wavelength λ and temperature T:

$$L_\lambda(\lambda,T)=\varepsilon(\lambda,T)\cdot L_{\lambda B}(\lambda,T)$$

If grey body radiation is assumed the emissivity ε does not depend on wavelength and temperature.

$$L_\lambda(\lambda,T)=\varepsilon\cdot L_{\lambda B}(\lambda,T)$$

For example particles in flames can be described by a grey body radiator. The integration of $L_{\lambda B}$ results in the Stefan-Boltzmann law of radiation which relates the total radiance to the 4th power of temperature.

$$\mathrm{E}=\varepsilon\sigma T^4$$

ε depends on the concentration and size of the emitting particles, σ being the Stefan-Boltzmann constant. ε is very low for lean and small flames (≅ 0.0001) and close to 1 for large fires especially when containing many particles.

2-COLOR-PYROMETRY - COMPARISON OF GREY BODY RADIATION IN VIS AND NIR

The 2-color-pyrometry is a simple and very fast temperature measurement technique for gray body emission. It is assumed that ε is independent of wavelength and temperature. Therefore, it is restricted for black body, respectively gray body, radiators. The 2-color-pyrometer is composed of an electronics who records the signals of two photodiodes. The sampling frequency is between a few Hz up to some MHz in dependency of the sampling rate of the measuring electronics. The two photodiodes are in one package, constructed as a sandwich diode of silicon over InGaAs diode. The silicon diode is sensitive in the UV/Vis range from 400 nm till 1000 nm and the sensitivity of the InGaAs diode ranges from 1025 nm till 1700 nm. The construction as a sandwich diode guarantees that both diodes collect light from the same element of the measured radiation. The photodiode is adapted to the combustion process by an optical fiber. The temperature of a gray body radiation can be determined by the ratio of the irradiation in the UV/Vis and NIR/IR range. Due to the Wien´s law the maximum of a black body radiator shifts to smaller wavelength when increasing temperature and the ratio of UV/Vis to NIR/IR radiation increases. By analyzing the ratio of the photodiode signals, the temperature can be determined, if a calibration of the ratio was done before with a calibration standard like a technical black body or a tungsten strip lamp. Examples for measurements on pyrotechnic mixtures are found in literature [24]. Be careful if H_2O arise in the spectrum, the intensity in NIR/IR range (signal of the InGaAs diode) increases without change of gray body radiation and misleadingly the temperature signal changes.

NIR-SPECTROSCOPY – GREY BODY RADIATION IN THE NIR WAVELENGTH BAND

For spectroscopic temperature measurement in the UV/Vis/NIR wavelength band the spectrometer split the wavelength range not just in two ranges like the 2-color-pyrometer but in many channels. Therefore different types of spectrometers are available, like filter-wheel spectrometer for the wavelength range of 1.4 µm till 14 µm or grating spectrometer with a fixed grating, 256 channels, a wavelength range from 0.3 µm till 2.2 µm and a fiber optic entrance.

Hence the spectrometer uses many supporting points in the NIR wavelength range. After calibration with a black body radiator, the function of the gray body can be fitted by a least-squares fit to such an experimental spectrum [25][26]. The result is a gray body temperature with a temperature-independent emissivity. 2-color-pyrometer and spectrometer measurement techniques for gray body radiation measure the temperature of solid surfaces or in the gas phase of particles. Further applications are given in Ref. [27][28].

UV-VIS SPECTROSCOPY AT DIATOMIC MOLECULES – DIATOMIC BAND SPECTRA

In the UV/Vis wavelength range electronically excited atoms and diatomic molecules emit their species-specific radiation. The arising molecules can be identified by tabulated data from literature [46] and the temperature of the gas phase can be determined by band modelling of the diatomic molecule spectra, i.e. the calculation of the intensity distribution [29]. The calculated diatomic spectra are fitted to the experimental data by a least squares fit with the temperature being the only fit parameter. Calculation of spectra is based on quantum mechanical principles and uses the Born-Oppenheimer approximation for the energy, or wavelength, the Einstein coefficients for spontaneous emission for transition probabilities (dipole moments) and the intensities and a line profile. Needed molecular constants are available in literature for a number of molecules [18]. In the case of pyrotechnic mixtures diatomic molecules mostly intermediate products and oxides of metals are visible in the UV/Vis-spectrum, like AlO, AlH, Cu_2, CuO, MgO, MgH, TiO [21]. Here, the $B^2\Sigma$-$X^2\Sigma$-transition of the AlO molecule is discussed in detail. In the case of pyrotechnic mixtures containing aluminum it is nearly always visible.

The total energy of a molecule state is given by the Born-Oppenheimer approximation:

$$E_{tot} = E_{el} + E_{vib} + E_{rot}$$

It is the sum of electronic energy E_{el}, vibrational energy E_{vib} and rotational energy E_{rot}. The electronic energy is the sum of kinetic and potential energy of the electrons in the coulomb potential of the nuclei and so it is constant for a given electronic transition. For the vibrational energy first a harmonic oscillator is assumed. But the potential of a molecule state is not harmonic due to different perturbations and so different experimental inharmonic terms are added to the harmonic oscillator eigenvalues. The eigenvalues are:

$$E_{vib} = \omega_e\left(v+\frac{1}{2}\right) - x_e\omega_e\left(v+\frac{1}{2}\right)^2 + y_e\omega_e\left(v+\frac{1}{2}\right)^3 + \cdots$$

with: $\omega_e = \frac{1}{2\pi c}\sqrt{\frac{k}{\mu}}$ $\quad x_e\omega_c > 0$ and

v = vibrational quantum number; k = spring constant and µ = reduced mass. This equation is valid for all diatomic molecules.

For the calculation of the rotational energy different couplings of the angular momenta of the electrons (orbital angular momentum, spin), the nuclei (nuclear momentum) and the molecule must be taken into

account. The different coupling cases, called Hund's cases and the resulting eigenvalues for the rotational energy are discussed in detail in Ref. [29]. The rotational energy depends on the involved states of the electronic transition. During the rotation of the molecule also a centrifugal force occurs, which will be considered too.

For example, at the $B^2\Sigma$-$X^2\Sigma$-transition of the AlO molecule for both states coupling case b is valid and the expression for the rotational energy is given by:

$$F_{v,e}(J) = B_v J(J+1) - D_v J^2(J+1)^2 + \frac{\gamma}{2}\left(J - \frac{1}{2}\right)$$

$$F_{v,f}(J) = B_v J(J+1) - D_v J^2(J+1)^2 - \frac{\gamma}{2}\left(J + \frac{1}{2}\right)$$

J is the rotational quantum number. The appearance of spin doubling is included by γ and the centrifugal stretching of the rotation by D_v. The rotational constants are taken from Ref. [30][31][32]. The rotation-vibration interaction in all molecules is taken into account using an average value for the rotational constants B_v and D_v. This is possible under the assumption that the vibrations are much faster than the rotations. This approximation provides with the following constants [33]:

$$B_v = B_e + \alpha_e\left(v + \frac{1}{2}\right) + \cdots \text{ and } D_v = D_e - \beta_e\left(v + \frac{1}{2}\right) + \cdots$$

The intensities and transition probabilities are calculated with the Einstein-coefficients for spontaneous emission. The intensity of an emitting line is given by:

$$I_{nm}^{em} = N_n hc\nu_{nm} A_{nm}$$

With N_n = number of molecules in the excited state $N_n = \frac{Nd_u}{Z} e^{-\frac{hcE_{mol}^{'}}{k_B T}}$ and A_{nm} Einstein-Coefficient for spontaneous emission $A_{nm} = \frac{64\pi^4 \nu_{nm}^3}{3h}\left|R_{nm}\right|^2$ with R_{nm} matrix element of the transition. $hc\nu_{nm}$ is the energy of the emitted photon.

The matrix element R_{nm} for the electronic transition in Born-Oppenheimer approximation is given by:

$$R_{nm} = \int \Psi_{vib}(v'') R_{nm}^{el} \Psi_{vib}(v') dR \cdot \iint Y_{J''}^{n''} Y_{J'}^{n'} \sin\vartheta d\vartheta d\varphi$$

The first term provides in r-centroid approximation with the transition probability for the electronic and the vibrational transition [33].

$$S_{v''v'} = \left|R_{nm}^{el}(R_{v''v'})\right|^2 \cdot \left|\int \Psi_{v''} \Psi_{v'} dR\right|^2 = \left|R_{nm}^{el}(R_{v''v'})\right|^2 \cdot q_{v''v'}$$

The values are taken from References [34]. The square of the second term yields to the Hönl-London factors which are given in [35][36][37].

The line profile is a convolution of the Lorentz line profile (γ line width) due to the natural line width with additional dispersion mechanisms and the Gaussian profile (σ line width) of the spectrometer entrance slit.

Due to the fact that the Gaussian profile dominates the line profile ($\gamma/\sigma << 1$) a Gaussian profile was chosen for modelling the diatomic molecule spectra.

In the case of the copper diatomic molecules CuO ($A^2\Sigma$-$X^2\Pi$ transition) and Cu_2 ($A^1\Sigma$-$X^1\Sigma$ transition), the rotational energy levels and rotational constants are known and discussed in Ref. [38][39][40]. Unfortunately, the transition probabilities of the involved vibrational states were not calculated yet. To determine them, the transition probabilities of the vibrational bands (Franck-Condon factors) can be calculated from the potential energy curves. In turn the potential energy curves were calculated by the method of Rydberg-Klein-Rees (RKR-method) using the RKR1 2.0 Code by R. J. Le Roy [41]. The method was discussed in detail in Ref. [42]. Here, the resultant potential curves for $A^2\Sigma$-$X^2\Pi$ transition of CuO and $A^1\Sigma$-$X^1\Sigma$ transition of Cu_2 are depicted in Figure 1 from Ref. [43].

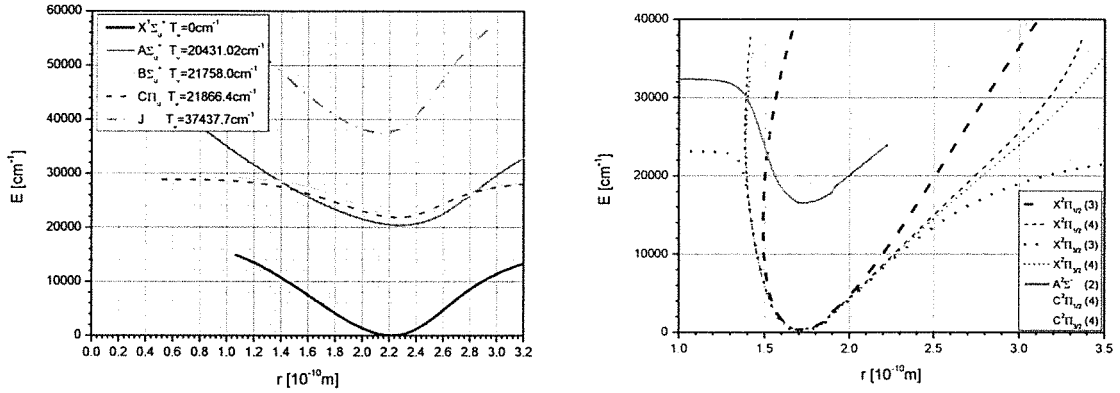

Cu_2 *CuO*

Figure 1: Calculated potential energy curves of the Cu_2 and CuO molecule.

The potential energy curves and the equilibrium distances of the Cu_2 molecule are in good agreement with Ref. [38]. For the CuO molecule they differ by a factor of two in comparison to [44]. From there the Franck-Condon factors were calculated by solving the 1-dimensional Schrödinger equation with the before calculated potential energy curves using the LEVEL 8.0 Code again by R. J. Le Roy [45]. For example, the transition probabilities of the $A^1\Sigma$-$X^1\Sigma$ transition of Cu_2 are listed in Table 1. The vibrational transition probabilities for CuO are listed in Ref. [43].

v'\v''	0	1	2	3	4	5
0	6.58143 e-01	2.13796 e-01	8.62145 e-02	2.87330 e-02	9.28075 e-03	2.77298 e-03
1	3.17659 e-01	2.43881 e-01	1.90100 e-01	1.40255 e-01	6.56741 e-02	2.76294 e-02
2	2.24293 e-02	4.73223 e-01	7.07032 e-02	1.09723 e-01	1.48270 e-01	9.26786 e-02
3	9.42308 e-04	6.28078e-02	5.24696e-01	1.19995e-02	4.26660e-02	1.26599 e-01
4	8.03881 e-04	2.65648 e-03	1.13994 e-01	5.14545 e-01	8.91042 e-05	7.20973 e-03
5	1.53435 e-07	3.50147 e-03	4.73926 e-03	1.68417 e-01	4.71815 e-01	2.23641 e-03

Table 1: Franck-Condon factors for the $A^1\Sigma$-$X^1\Sigma$ transition of Cu_2.

With the rotational constants from [38], the calculated Franck-Condon factors and a line profile the emission spectra for different temperatures can be calculated [43] shown in Figure 2 for Cu_2 and CuO.

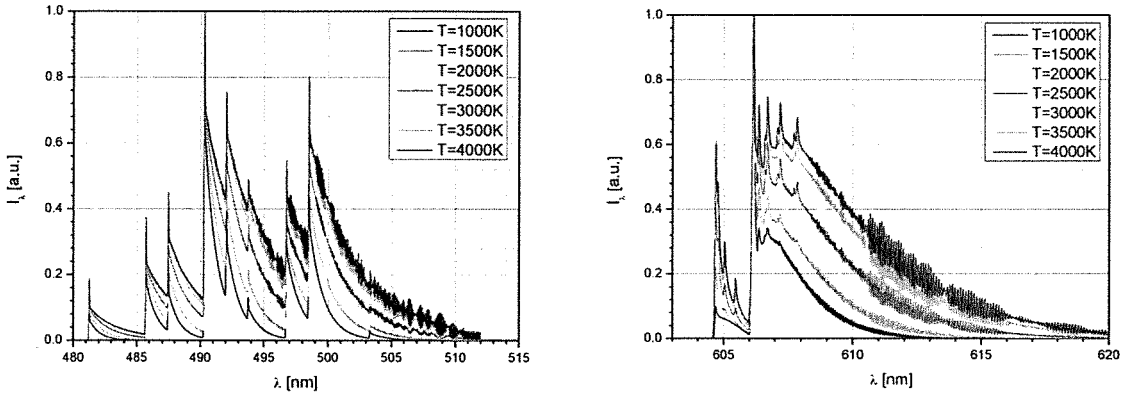

Cu_2 CuO

Figure 2: Calculated emission spectra of Cu_2 $A^1\Sigma$-$X^1\Sigma$ and CuO $A^2\Sigma$-$X^2\Pi_{3/2}$ for different temperatures.

Examples of the calculated spectra of AlO with marked rotational branches are shown in Figure 3 for a temperature of 3000 K.

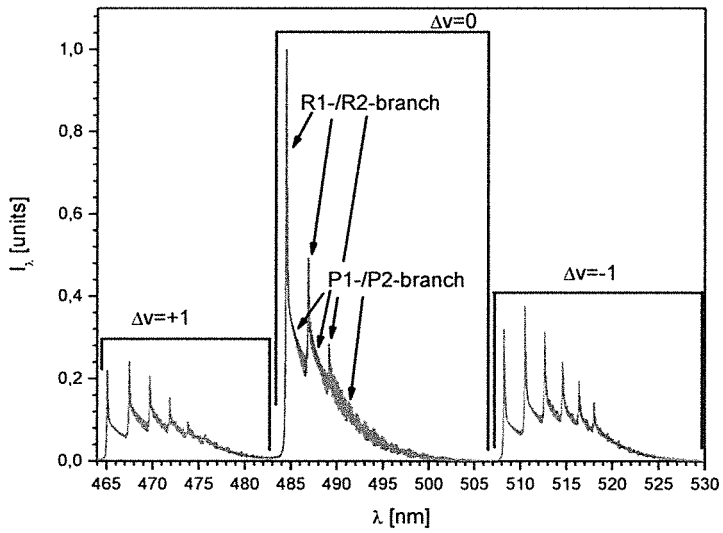

Figure 3: Calculated emission spectrum of AlO $B^2\Sigma$-$X^2\Sigma$ system.

LINE INTENSITIES

For information about the transient occurrence of intermediate and reaction products the intensities of the atomic lines and integral intensity of diatomic molecule band systems can be analyzed. Therefore, overview spectra of the UV/Vis range with measured spectra in the gas-phase of the reaction were used. First, the emitting lines and band-systems of the diatomic molecules in the spectra were identified using [46]. Of main interest were the intensities of the atomic lines of the involved elements (Al, Cu at Al/CuO-thermite) and of the resulting diatomic molecules (AlO, CuO, Cu_2 at Al/CuO-thermite). First the background radiation caused by the radiation of the glowing melts or hot particles must be subtracted. The background corrections were done by zoom in the spectra at the interesting wavelength and approximate a linear background. After that procedure the integral intensity was calculated. The integral intensities were normalized for better comparison of each other.

CIE COLOR VALUES

The CIE color values create a relation between human color perception and physical cause of color stimulation. The method was developed from the international commission on illumination (CIE – Commission internationale de l'éclairage) in 1931 with the outcome of the CIE color space chromaticity diagram [47]. A new definition was done in 1964, but still the definition from 1931 is more common. By physical color re-creation they developed weight functions for the fundamental colors red, green and blue. The aim was mathematical-captured human color perception. Therefore, the measurement values were related to a standard observer to represent an average human chromatic response within a 2° arc (1931) or 10° arc (1964) inside the fovea. The weight functions were defined for a wavelength range from 380 nm till 780 nm, in 1, 5, 10 and 20 nm steps. Today wavelength step width of 0.1 nm is achieved by interpolation. The CIE color value, also known as XYZ color values, can be calculated from emission spectrum by multiplication of the weight functions for red $\bar{x}(\lambda)$, green $\bar{y}(\lambda)$ and blue $\bar{z}(\lambda)$ with the spectral power distribution $P(\lambda)$. The spectral power distribution equates the calibrated emission spectrum, where also a relative calibration is sufficient. After multiplication the functions are integrated or the sum is formed:

$$X = k\int_{380}^{780} \bar{x}(\lambda)P(\lambda)d\lambda \quad \text{or} \quad X = k\sum_{\lambda} \bar{x}(\lambda)P(\lambda)\Delta\lambda$$

$$Y = k\int_{380}^{780} \bar{y}(\lambda)P(\lambda)d\lambda \quad \text{or} \quad Y = k\sum_{\lambda} \bar{y}(\lambda)P(\lambda)\Delta\lambda$$

$$Z = k\int_{380}^{780} \bar{z}(\lambda)P(\lambda)d\lambda \quad \text{or} \quad Z = k\sum_{\lambda} \bar{z}(\lambda)P(\lambda)\Delta\lambda$$

If the constant k is chosen in the way, that the values X, Y, Z are in units of the luminance, X, Y and Z are called absolute CIE-values. In this case, $k = 683\ lm\ W^{-1}$. Therefore, the spectral power distribution must be also in units of $[W\ m^{-2}\ sr^{-1}\ nm^{-1}]$ and a relative calibration of the emission spectra is not sufficient.

The XYZ values are represented in two dimensional diagrams, the CIE chromaticity diagram, where the Z component is calculated from the X and Y component by normalization

$$x + y + z = 1$$

The values x, y, z are the normalized values of the XYZ values. They are calculated by

$$x = \frac{X}{X+Y+Z}$$

$$y = \frac{Y}{X+Y+Z}$$

$$z = \frac{Z}{X+Y+Z}$$

Therefore, the normalization of the XYZ values (constant k) doesn't matter. An example for the CIE chromaticity diagram is shown in Figure 4.

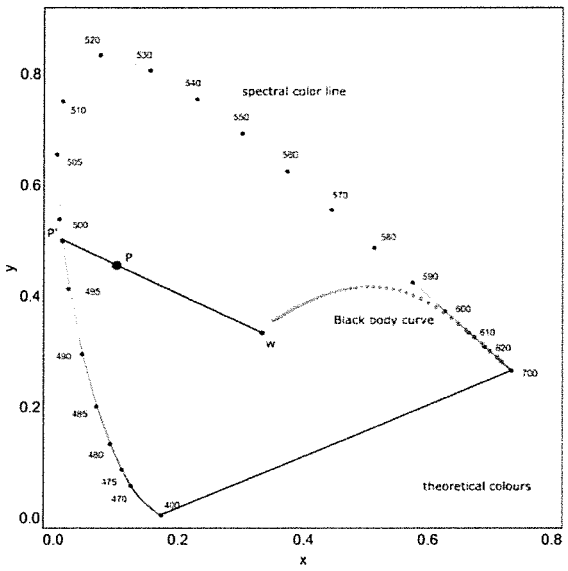

Figure 4: The CIE chromaticity diagram with the spectral colour line, the white point W, an example colour point P and its dominant wavelength P'.

Experimental

Some of the shown examples below were ignited in a fume hood but most of them were burned in a high pressure autoclave, called window bomb. The window bomb is a metallic cylinder with two opposite optical quartz windows (V = 1.2 L), in which a flow is generated. Pressures up to 15 MPa can be realized under different atmospheres, for example oxygen, nitrogen and synthetic air. The samples were burned as bulk material on a glass plate in synthetic air or nitrogen under a pressure of 0.1 MPa. Sample mass was mostly about 1 g. For detailed information of the experimental setup with the window bomb see Figure 5 and Ref. [48]. Experiments in the fume hood are described in detail in Ref. [49].

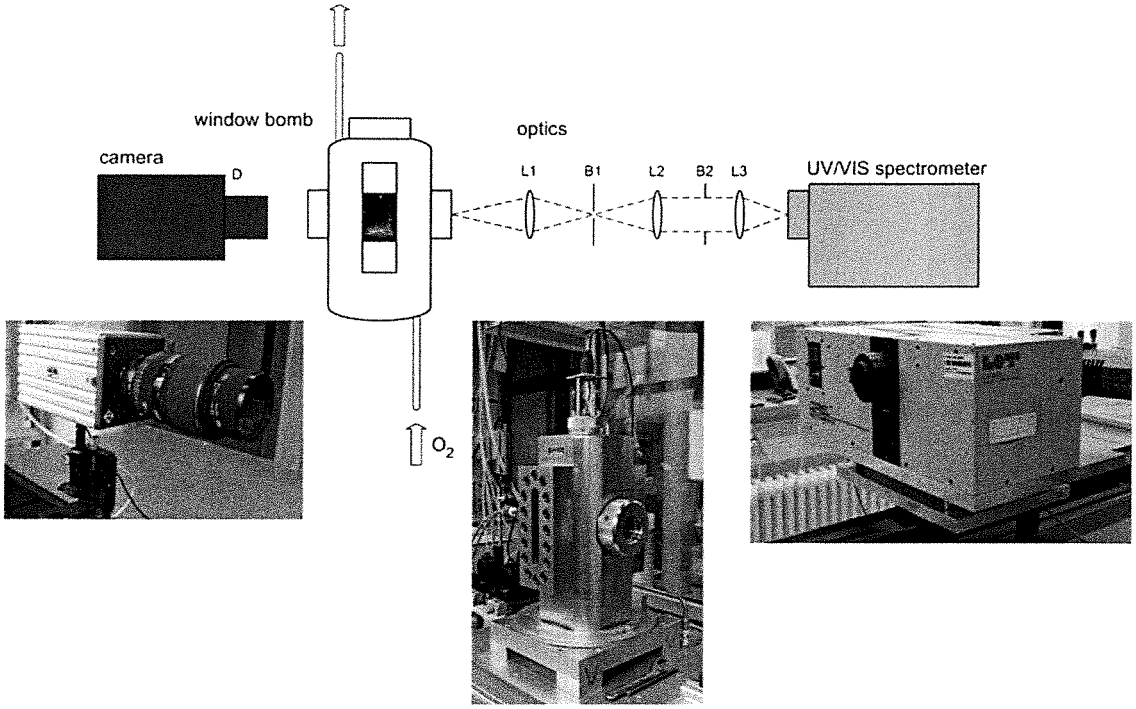

Figure 5: Experimental setup window bomb.

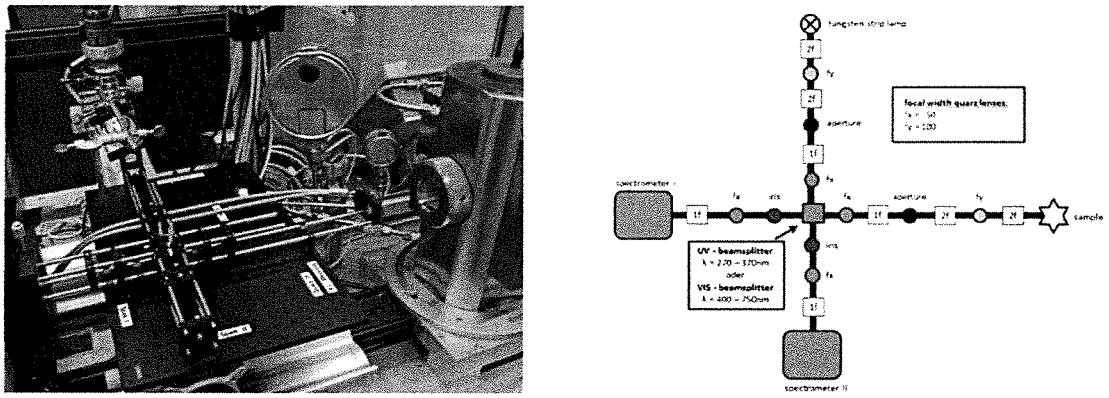

Figure 6: Optical setup at the window bomb.

The UV/Vis emission of the combustion process was imaged with an optical quartz lens system to the entrance slit of the spectrometer (20 µm). The aperture (diameter 1 mm) in the optical path reduces the field of view of the spectrometer to the emission of the vapor phase of the combustion zone. The optical setup at the window bomb is depicted in Figure 6. It consists of two identical optical paths which are both coupled to the spectrometer by the beam splitter. One path observes the experiment and the other one the calibration lamp. Therefore, it is not necessary to modify the experimental setup for calibration, only switch on the calibration lamp for calibration and switch it off for measuring (Figure 6).

The used spectrometer is a UV/Vis grating imaging spectrometer in Czerny-Turner-arrangement with a focal length of 498 mm (Andor Shamrock A-SR500i B2). Six different gratings are available with different resolutions. Gratings with 1200 l/mm and different blaze angles were used to cover the wavelength range from 200 to 900 nm. The spectrometer is coupled to a Si-CCD-camera with

256 x 1024 pixels and a maximum speed of 1000 spectra/s in full vertical binning mode (Andor CCD DU920P-UV-BR-DD). Mercury-argon and neon lamps were used to calibrate the wavelengths of the spectra. To correct the intensity distribution for the different sensitivities of the gratings and the CCD-camera pixels for different wavelengths, a tungsten strip lamp with a defined radiation capacity was used with the setup described above.

Furthermore a low-resolution fixed grating UV/Vis/NIR-spectrometer with a wavelength range from 300 till 2140 nm, a maximum wavelength resolution of 18 nm and a maximum speed of 60 spectra/s was coupled to the bomb window by an optical fibre. The second window of the window bomb was equipped with a high-speed camera (MotionPro X3 from Redlake) with a resolution of 2000 fps (at 1280 x 1024 pixels) for the observation of the combustion process.

Results

In this work an Al/CuO thermite with micron-sized particles and a mixture ratio of 30:70 wt.-% was investigated in the window bomb and in a fume hood. The emitted light of the combustion process was observed by the different emission spectrometer. An overview spectrum is shown in Figure 7 and highly resolved spectra of the visible range with the atomic lines and diatomic band systems of interest are shown in Figure 8. Between 460 – 550 nm the atomic lines of Copper, the AlO $B^2\Sigma$-$X^2\Sigma$, the Cu_2 $A^1\Sigma$-$X^1\Sigma$ and $B^1\Sigma$-$X^1\Sigma$ system could be definitely identified by comparison with literature values and calculated spectra [43].

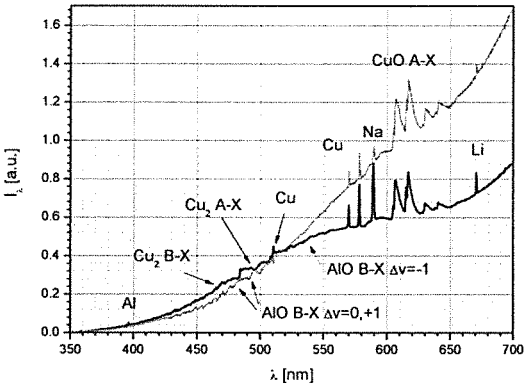

Figure 7: Overview spectra of Al/CuO thermite combustion.

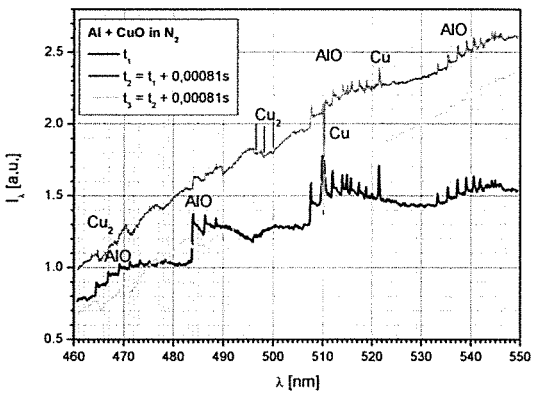

Figure 8: Highly resolved spectra of the Al/CuO combustion in the range 460-550 nm.

CONTINUUM TEMPERATURES - ABSOLUTE CALIBRATED INTENSITY

Combustion of pyrotechnic mixtures forms normally a hot melt and hot particles. They emit a grey body radiation which can be detected in the whole wavelength range from UV/Vis, NIR till IR. We observed the combustion process with an NIR spectrometer and determined the temperature with a fit of a grey body radiation function (see Figure 9). It ranges from 2000 K at the beginning till 1200 K at the end of the process after 0.08 s. The process itself takes only 0.08 s because of the small sample mass. In parallel the combustion process was observed with in the UV/Vis range by the emission grating spectrometer and the color high-speed camera. The intensity of each frame of the high-speed camera video was summarized in one line and the lines were put together to a new picture. The new picture shows the integral intensity in height (y-coordinate) over time (x-coordinate) (see Figure 11). By the optical setup described above, the spectrometer can be calibrated absolutely by the tungsten strip lamp. The result is a y-axis with units of

$Wm^{-2}nm^{-1}sr^{-1}$. Therefore, the absolute emissivity and the continuum temperature of the combustion process at the measurement point of the optical setup can be determined by fitting a grey body function to the experimental spectra. A result of the combustion of the Al/CuO thermite is shown in Figure 10 (black = continuum temperature, red = emissivity). The determined emissivity is between 0.002 at the beginning and up to 0.57 at the two peaks after 0.0025 s and 0.005 s. The two peaks can additionally be correlated with the two bright strips in the analyzed high-speed video picture (Figure 11).

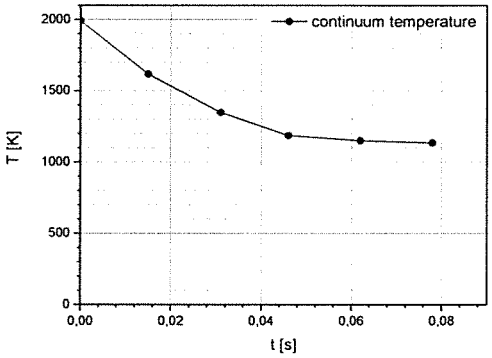

Figure 9: Determined continuum temperature in the NIR range.

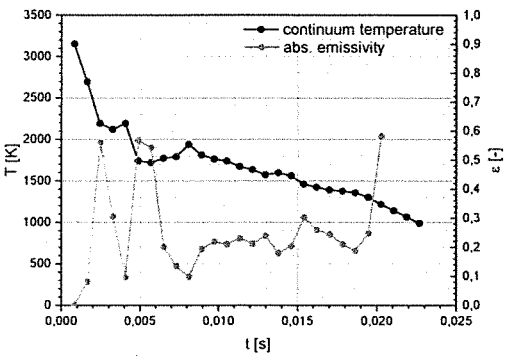

Figure 10: Determined continuum temperature and emissivity in the UV/Vis range.

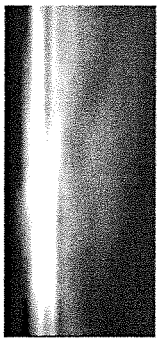

Figure 11: Result of the high-speed video.

With the continuum temperature and the emissivity, the radiated energy at the measurement point can be calculated with the Stefan-Boltzmann-Law. For calculation of the radiated energy of the whole combustion process the geometry of the flame and the temperature and emissivity at each point in the flame must be known. Determination of the temperature and emissivity profile over the whole flame is therefore a special challenge.

GAS PHASE TEMPERATURE

The gas phase temperature can be determined by modelling the spectra of the observable diatomic molecule bands and fit them to experimental one. In the case of Al/CuO thermite sometimes the Cu_2 $A^1\Sigma$-$X^1\Sigma$ system overlays with the AlO system or it is in absorption, so that temperature determination by fitting the calculated spectrum of Cu_2 or AlO to the experimental one is impossible (Figure 12). The overlay factor (0.25) of the calculated spectra (blue line) was arbitrarily selected. The band head of the AlO $B^2\Sigma$-$X^2\Sigma$ system with $\Delta v=0$ vibrational band do not overlay and for this small wavelength range from 483.9 – 486 nm a fit (FWHM = 0.065 nm) was possible. This is acceptable because the sloping edges of AlO vibrational transitions are very temperature sensitive [49]. The obtained temperature for the vapor phase on the basis of the AlO molecule was between 2500 K and 3250 K.

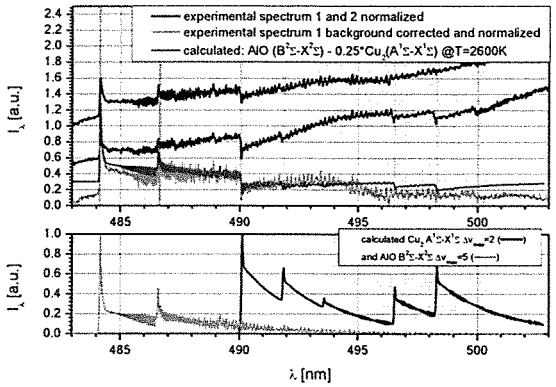

Figure 12: Illustration of the overlaying spectra of AlO and Cu_2.

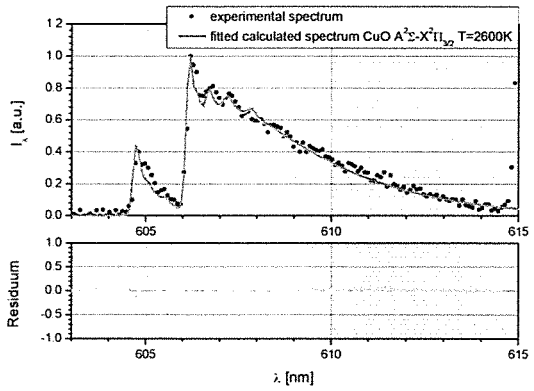

Figure 13: Fit of the calculated to an experimental spectrum of the CuO $A^2\Sigma$-$X^2\Pi_{3/2}$ subsystem.

In the wavelength range from 603 – 621 nm the CuO $A^2\Sigma$-$X^2\Pi$ system appears with no overlay. In a first step the $A^2\Sigma$-$X^2\Pi_{3/2}$ subsystem was calculated and fitted to the experimental spectra (Figure 13). The determined temperature for the vapor phase on the basis of the CuO molecule was between 2500 K and 2750 K nearly constant over time and in good agreement with the temperature of the AlO molecule.

LINE INTENSITIES

The UV/Vis overview spectra of the Al/CuO mixture feature in a variety of emitting atomic lines and systems of diatomic molecules which are identified in Figure 14. Clearly visible are the Al-lines at 394.4 and 396.2 nm further lines at 308.2 and 307.3 nm are weak. Significant copper lines were found at 570 and 578.2 nm and at and 324.7 and 327.4 nm. Distinct band systems of the diatomic molecules are evident of AlO in the range 445 to 555 nm and CuO at 605 to 645 nm. In air the line respectively the band integral intensities were determined as shown in Figure 15. The profiles are normalized to 1 for maximum intensity.

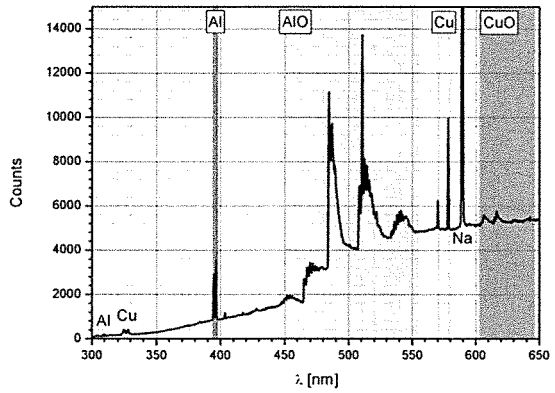

Figure 14: Overview spectrum of the Al/CuO thermite with identified lines and band-systems.

The reaction starts with a short highly intense emission of about 50 ms. Here all considered species feature their maximum intensity. First, CuO rise up directly followed by Cu. The increase of Al and AlO is little slower and these species reach their maximum intensity about 10 ms later. At this time Cu and especially CuO are already decreasing strongly. Then the signals of Al, Cu and AlO start to resonate with a large damping and decreasing frequency. After 0.4 s their intensities converge to nearly zero but are still apparent up to 0.7 s. The integral intensity of the CuO diatomic molecule also resonates with a large

damping but out–of-phase with the other three species. It has his maximum when all other species have a minimum and vice versa.

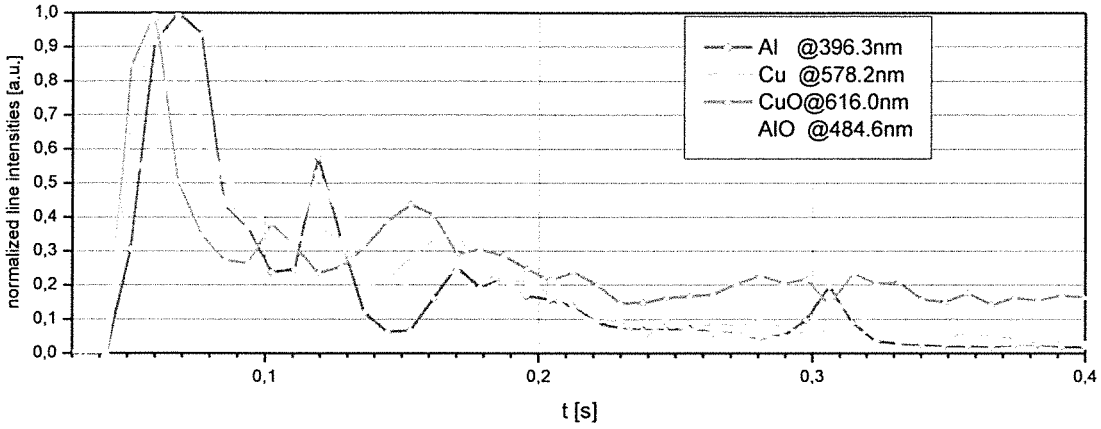

Figure 15: Integral intensities of the Al- and Cu-lines and the AlO- and CuO band-systems in nitrogen.

CIE COLOR VALUES

From the UV/Vis spectra of the Al/CuO thermite the CIE color values can be calculated for an objective quantification of the luminous color of the combustion process. In Figure 16 one spectrum and in Figure 17 the corresponding color value are depicted. In the emission spectrum the atomic lines of aluminum, copper and sodium and the diatomic bands of AlO overlaid with Cu_2 and CuO are visible which results in a CIE color value of x = 0.4, y = 0.47 and z = 0.14 with a dominant wavelength of 568 nm. All other spectra of a series show similar CIE values with a shift to the black body curve in the CIE chromaticity diagram (compare Figure 4 and Figure 17).

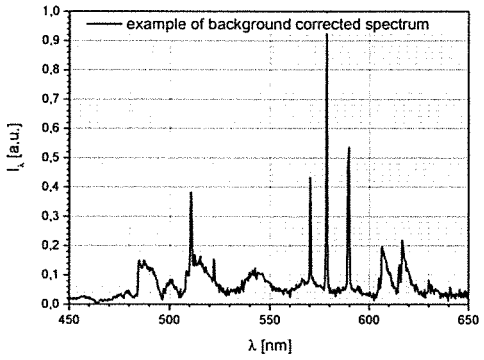

Figure 16: Example spectrum of the Al/CuO thermite for CIE color value determination.

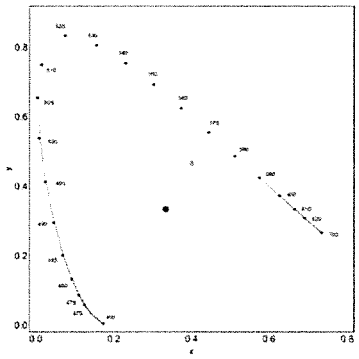

Figure 17: The determined color value of the UV/Vis spectrum (left) of the Al/CuO thermite.

Conclusion

Emission spectroscopy in the UV/Vis wavelength range provides a lot of information about the combustion of pyrotechnic mixtures and helps for a better understanding of the combustion process. In this work, the different methods of data analyzing are shown and examined using the example of an Al/CuO thermite mixture. From radiation of hot surfaces, melt and particles in the NIR range the

continuum temperature can be determined by fitting a grey body function. The grey body radiation is also visible in the UV/Vis range and again the continuum temperature is received from the spectrum. By an absolute calibration of the spectrometer sensitivity not only the continuum temperature but also the emissivity is calculated and therefore, the radiated energy at the measurement point can be calculated. For the example system of an Al/CuO thermite in the UV/Vis range continuum temperatures between 3000 K and 1000 K are obtained which are in good agreement with the NIR continuum temperature. The determined emissivity is between 0.002 at the beginning up to 0.57 at the two peaks after 0.0025 s and 0.005 s.

In the UV/Vis range, the temperature of the vapor phase can be determined from the band systems of arising diatomic molecules. During the combustion of Al/CuO thermite, AlO, Cu_2 and CuO were observed and spectral intensities determined by calculation of the first excited transitions of the diatomic copper compounds Cu_2 and CuO. Their potential energy curves and the vibrational transition probabilities were calculated from the diatomic constants given in the literature. With a fit of the calculated to the experimental spectra the temperature of the vapor phase of the burning Al/CuO thermite was determined between 2500 K and 3250 K. The adiabatic temperature of the substoichiometric thermite mixture of 30% Al and 70% CuO was calculated with the EKVI-Code to $T_{adiabatic} = 2540$ K [51]. The measured higher temperature may result from a gas-phase reaction of Al + O → AlO. Oxygen might derive from decomposing copper oxide. For this reaction the adiabatic temperature is much higher with $T_{adiabatic} = 3700$ K.

The time-dependent wavelength-integrated line intensities gives a hint to the reaction behavior of the combustion. In the case of the Al/CuO thermite Cu-lines and CuO bands arises before the Al and AlO bands are visible. The integral intensity of the CuO diatomic molecule also resonates with a large damping but out-of-phase with the other three species. It has his maximum when all other species have a minimum and vice versa. Although the time resolution is not high enough, the series seems to give reason for the assumption of a thermite reaction, where first the oxide is decomposed before the oxidation of the fuel occurs.

Pictures from the reaction of the Al/CuO thermite at different points in time are shown in Figure 18. Here, the development of the reaction process and the formation of the large volume of the vapor phase are visible. Near the boundary surface of the vapor phase a green region is observable which gives a hint for the formation of AlO and Cu_2 in the vapor phase. The orange/red color may be emitted from the dispersed copper formed by the reaction from aluminum with the copper oxide or from the emission of the $A^2\Sigma$-$X^2\Pi$ system of CuO. Furthermore the calculated CIE color values fits very well to the color impression of the pictures.

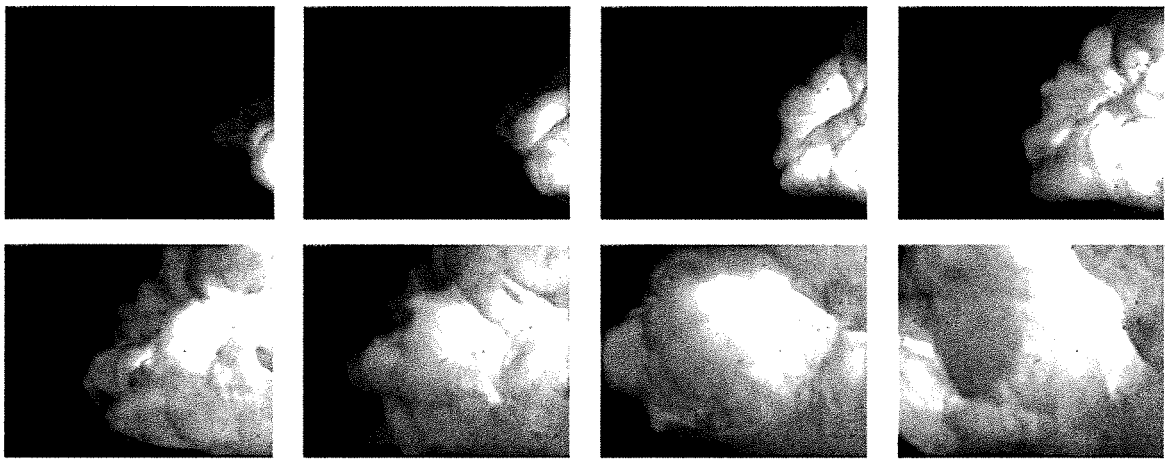

Figure 18: Time development of the Al/CuO thermite combustion.

References

[1] L. L. Wang, Z. A. Munir, Y. M. Maximov, Review Thermite reactions: their utilization in the synthesis and processing of materials, Journal of Material Science, 28, 3693-3708, 1993.

[2] Fischer S. H., Grubelich M. C.: Theoretical Energy Release of Thermites, Intermetallics, and Combustible Metals, 24th International Pyrotechnics Seminar, Monterey, California, USA, 27-31 July, 1998.

[3] C. P. Lonsdale, Thermite Rail Welding: History, Process Developements, Current Practices And Outlook For The 21st Century, Conrail Technical Services Laboratory Altoona, PA 16601

[4] O. Odawara, J. Ikeuch, Vacuum Centrifugal-Thermite Process for Producing Ceramic-Lined Pipes, J. Am. Ceram. Soc., 69 141 C-854-86, 1986.

[5] V. Weiser, E. Roth, S. Kelzenberg, W. Eckl, Pyrotechnic Incendiaries to Combat Toxic Clouds, 40th International Annual Conference of ICT, June 24 – 26, 13(1-12), 2009.

[6] D. Meerov, D. Ivanov, K. Monogarov, N. Muravyev, A. Pivkina, Y. Frolov, Mechanical Activation of Al/MoO3 Thermite as a Component of Energetic Condensed Systems to Increase Its Efficiency, Central European Journal of Energetic Materials, 6(3-4), 277-289, 2009.

[7] K. Ilunga, O. del Fabbro, L. Yapi, W. W. Focke, The effect of Si–Bi2O3 on the ignition of the Al–CuO thermite, Powder Technology 205, 97–102, 2011.

[8] M. L. Pantoya, J. J. Granier, Combustion Behavior of Highly Energetic Thermites: Nano versus Micron Composites, Propellants, Explosives, Pyrotechnics, 30, 53-62, 2005.

[9] M. R. Weismiller, J. Y. Malchi, R. A. Yetter, T. J. Foley Dependence of flame propagation on pressure and pressurizing gas for an Al/CuO nanoscale thermite, Proceedings of the Combustion Institute 32, 1895–1903, 2009.

[10] G. V. Ivanov, V. G. Surkov, A. M. Viktorenko, A. A. Reshetov and V. G. Ivanov, Nomalous dependence of the combustion rate of thermite mixtures on the pressure, Combustion, Explosion, and Shock Waves, 15, 266, 1979.

[11] Yajing Peng, Yinghui Wang, B. Palpant, Xing He, Xianxu Zheng, Yanqiang Yang,, Modeling heat-induced chemical reaction in nanothermites excited by pulse laser: a Hot-Spot-Model, International Journal of Modern Physics B 24, 381-395, 2010.

[12] S. Kelzenberg, V. Weiser, E. Roth, N. Eisenreich, B. Berger, B. Haas, Hot Spot Modeling of Thermite Type Reactions Regarding Particle Size and Composition; EuroPyro 2007 (9ième Congrès International de Pyrotechnie du GPTS) and the 34th International Pyrotechnics Seminar, October 8th – 11th 2007, Beaune, France, Proceedings by GTPS (Groupe de Travail de Pyrotechnie, France and the International Pyrotechnics Society,Vol. 1, pages 81 to 796, 2007.

[13] V. Weiser, S. Kelzenberg, N. Eisenreich, Influence of Metal Particle Size on the Ignition of Energetic Materials, Propellants, Explosives, Pyrotechnics 26, 284-289, 2001.

[14] G. Langer, N. Eisenreich, Hot Spots in Energetic Materials, Propellants, Explosives, Pyrotechnics, 24, 113-118, 1999.

[15] N. Eisenreich, T. S. Fischer, G. Langer, S. Kelzenberg, V. Weiser, Burn rate models for gun propellants, Propellants, Explosives, Pyrotechnics 27, 142-149, 2002.

[16] S. Knapp, V. Weiser, S. Kelzenberg, N. Eisenreich, Modeling Ignition and Thermal Wave Progression in Binary Granular Pyrotechnic Compositions, Propellants, Explosives, Pyrotechnics, 39, 423-433, 2014.

[17] H. S. Carslaw, J. C. Jaeger, Conduction of Heat in Solids, 2nd ed., Clarendon Press, Oxford, UK 1973.

[18] K. P. Huber, G. Herzberg, Molecular Spectra and Molecular Structure, Springer Science+Business Media New York, 1979.

[19] W. Eckl, N. Eisenreich, Temperaturbestimmung in heißen Gasen durch Analyse zweiatomiger Molekülspektren, ICT-Bericht 12/91.

[20] W. Eckl, N. Eisenreich, Determination of the Temperature in a Solid Propellant Flame by Analysis of Emission Spectra, Propellants, Explosives, Pyrotechnics 17, 202, 1992.

[21] Knapp, S., Emissionsspektroskopie an Flammen brennender Metalle; diploma thesis at Albert-Ludwigs-University, Freiburg im Breisgau, Germany, Sept. 2010.
[22] S. Knapp, W. Eckl, S. Kelzenberg, V. Weiser, Temperature determination analysing emission spectra of di-atomic metal oxides, 41st International Annual Conference of ICT: Energetic Materials for High Performance, Insensitive Munitions and Zero Pollution, Proceedings, June 29 – July 2, 2010 Karlsruhe, Germany, 80-(1-15).
[23] M. F. Modest, Radiative Heat Transfer, Academic Press, San Diego, California, 2003.
[24] N. Eisenreich, H. H. Krause, A. Pfeil, K. Menke, Burning Behaviour of Gas Generators with High Boron Content, Propellants, Explosives, Pyrotechnics 17, 161-163, 1992.
[25] V. Weiser, N. Eisenreich, Fast emission spectroscopy for a better understanding of pyrotechnic combustion behaviour, Propellants, Explosives, Pyrotechnics 30, 67-78, 2005.
[26] W. Eckl, N. Eisenreich, W. Liehmann, H. Schneider, and V. Weiser, Emission Spectroscopy and Pyrometry of Propellant Flames and Rocket Plumes, in: K. K.Kuo,T. P Parr (Eds), Non-Intrusive Combustion Diagnostics, Begell House Inc. New York, pp. 253, 1994.
[27] A. Blanc, N. Eisenreich, H. Kull, and W. Liehmann, Charakterisierung von Verbrennungsprozessen mittels Zeitaufgelöster IR-Spektroskopie im Bereich 1 – 14 µm, 19th Int. Annual Conference of ICT, Karlsruhe, Germany, June 29 – July 1, pp. 74/1, 1988.
[28] M. Hund, N. Eisenreich, F. Volk, Determination of Interior Ballistics Parameters of Solid Propellants, 77-84, 6th International Symposium on Ballistics 1981. Proceedings Arlington/Va.: ADPA, 1981.
[29] G. Herzberg, Molecular Spectra and Molecular Structure I. Spectra of Diatomic Molecules, D. van Nostrand Company Inc., Princeton, New Jersey, 1950.
[30] J. A. Coxon, S. Naxakis, Rotational Analysis of the $B^2\Sigma^+$-$X^2\Sigma^+$ System of the Aluminium Monoxide Radical, AlO, J. Mol. Spec. 111, 102-113, 1985.
[31] M.D. Saksena et. al., Fourier transform spectral study of $B^2\Sigma^+$-$X^2\Sigma^+$ system of AlO, J. Mol. Spec. 247, 47-56, 2008.
[32] M D Saksena, G S Ghodgaonkar and M Singh, The $B^2\Sigma^+$-$X^2\Sigma^+$ system of AlO, J. Phys. B: At. Mol. Opt. Phys. 22, 1993-1996, 1989.
[33] W. Demtröder, Molekülphysik, Oldenburg Wissenschaftsverlag GmbH, 2003.
[34] M. Singh, J. P. Chaturvedi, Some vibrational bands of B-X system of AlO molecule in the sun spectra, Bulletin Astronomical Society of India, 14, 175-179, 1986.
[35] I. Kovacs, Rotational Structure in the Spectra of Diatomic Molecules, Adam Hilger Ltd., London, 1969.
[36] R. J. M. Bennett, Hönl-London factors for doublet transitions in diatomic molecules, Mon. Not. R. astr. Soc., 147, 35-46, 1970.
[37] A. Schadee, The formation of molecular lines in the solar spectrum, B. A. N. Astronomical Institutes of the Netherlands, 5, 311-357, 1964.
[38] Page, R. H., Gudeman, C. S.: Rotationally resolved dicopper (Cu_2) laser-induced fluorescence spectra, J. Chem. Phys., 94 (1), 39-51, 1991.
[39] Appelblad, O., Lagerqvist, A.: The Spectrum of CuO: Rotational Analysis of Some Blue and Red Bands, Physica Scripta, 10, 307-324, 1974.
[40] Jin Jin, Ran Qin, Zhang Xiao-Peng, Chen Yang, Chen Cong-Xiang: Investigation of the $A^2\Sigma^-$ state of CuO by laser-induced fluorescence, Chinese Physics, 11, 5, 481-485, May 2002.
[41] Le Roy, R. J.: RKR1 2.0: A Computer Program Implementing the First-Order RKR Method for Determining Diatomic Molecule Potential Energy Curves, University of Waterloo Chemical Physics Research Report CP-657R, see http://leroy.uwaterloo.ca, 2004.
[42] S. M. Kirschner, J. K. G. Watson, RKR Potentials and Semiclassical Centrifugal Constants of Diatomic Molecules, Journal of Molecular Spectroscopy, 47, 234-242, 1973.
[43] S. Knapp, W. Eckl, S. Kelzenberg, A. Raab, E. Roth, V. Weiser, Emission spectroscopy on Al/CuO thermite mixture, 39th International Pyrotechnics Seminar, 2013.

[44] Daoudi, A., Benjelloun, A., T., Flament, J., P., Berthier, G.: Potential Energy Curves and Electronic Structure of Copper Nitrides CuN and CuN+ versus CuO and CuO+, Journal of Molecular Spectroscopy, 194, 8-16, 1999.

[45] Le Roy, LEVEL 8.0: A Computer Program for Solving the Radial Schrödinger Equation for Bound and Quasibound Levels, University of Waterloo Chemical Physics Research Report CP-663, see http://leroy.uwaterloo.ca/programs, 2007.

[46] R. W. B. Pearse, A. G. Gaydon, The identification of molecular spectra, Fourth Edition, Chapman and Hall Ltd., London, 1976.

[47] F. Grum, C. J. Bartleson, Optical Radiation Measurements Volume 2 Color Measurement, Academic Press, New York, 1980.

[48] O. Schulz, V. Weiser, J. Neutz, E. Roth, A. Raab, W. Eckl, Cinematographic and Spectroscopic Investigation of the Combustion of Aluminum, Titanium and Boron with Oxygen, 39th International Annual Conference of ICT: Energetic Materials Processing and Product Design; June 24 - June 27, 2008; Karlsruhe; Germany; 118-(1-11).

[49] S. Knapp, V. Weiser, W. Eckl, Time resolved UV/Vis-spectroscopy on thermite reactions, 43rd International Annual Conference of ICT: Synthesis, Characterization, Processing, June 26 – June 29, 2012, Karlsruhe, Germany, 68-(1-13).

[50] Knapp, S., Eckl, W., Kelzenberg, S., Koleczko, A., Raab, A., Roth, E., Steinert, S., Weiser, V.: Emission Spectroscopy on Wire Explosions in Different Atmospheres, Proceedings of the HEMs 2011, La Rochelle, France, 2011.

[51] B. Noläng, Ekvi System 3.2, BeN Systems, Balinge, Sweden, 2004.